encit 2020

ABCM
Associação Brasileira de Engenharia e Ciências Mecânicas

18th Brazilian Congress of Thermal Sciences and Engineering
November 16–20, 2020, (Online)

ENC-2020-0214
BLOOD FLOW NUMERICAL SIMULATION USING ALE-FE METHOD FOR VORTICITY-STREAMFUNCTION FORMULATION

Leandro Marques
Jose Pontes
State University of Rio de Janeiro - UERJ, R. Fonseca Teles 524, Rio de Janeiro, Brazil
marquesleandro.uerj@gmail.com and jose.pontes@uerj.br

Gustavo R. Anjos
COPPE/Federal University of Rio de Janeiro - UFRJ, R. Horacio Macedo, 2030, Rio de Janeiro, Brazil
gustavo.rabello@coppe.ufrj.br

Abstract. *The present work aims at developing a computational framework to simulate blood flow in coronary artery with drug-eluting stent placed using Streamfunction-Vorticity Formulation in a ALE-FE approach with Semi-Lagrangian Scheme. The blood was modeled as single-phase, incompressible and newtonian fluid and the Navier-Stokes equation in an Arbitrary Lagrangian-Eulerian description (ALE) is shown according to the stream-vorticity formulation with species transport equation. The Finite Element Method (FEM) is used to solve the governing equations where the Galerkin formulation was used to discretized the equations in space and the semi-Lagrangian scheme was used to discretized the material derivative using first order backward difference scheme. The linear systems was solved using Conjugate Gradient Method and the preliminary results are shown.*
Keywords: *Stream-Vorticity, Finite Element Method, Semi-Lagrangian, Drug-Eluting Stent, Arbitrary Lagrangian-Eulerian.*

1. INTRODUCTION

According to the World Health Organization (2017), more people die annually from the cardiovascular disease (CVD) that from any other cause in the world. An estimated 17.9 million people died from CVD in 2016, representing 31% of all global deaths. About 44% of these deaths were due to coronary heart disease (CHD) in the United States (Benjamin *et al.*, 2018). According to the Barquera *et al.* (2015), the leading cause of the CHD is atherosclerosis where the diameter of the vessel is decreased and the best treatments is the lifestyle change. For a corrective approach, however, two treatments can be performed: coronary artery bypass grafting (CABG) or percutaneous transluminal coronary angioplasty (PTCA). The PTCA is a minimally invasive procedure where a small wire tube, called stents, is placed. This work aims to develop an ALE-FE code for stream-vorticity formulation with species transport equation using semi-Lagrangian scheme and to know how occurs the dynamics of blood flow in coronary artery with atherosclerosis and with stents struts placed.

The dynamics of blood flow in coronary artery and possible influence of stents struts with computational fluid dynamics (CFD) requires a robust numerical method to compute the solution of the differential equations in a relevant model. The equations that govern the dynamics of blood flow in a coronary artery were developed according to continuum media assumption. Thus, the universal conservation laws such as conservation of mass, conservation of momentum and conservation of species transport were used in an Arbitrary Lagrangian-Eulerian context. The blood was modeled as single-phase, incompressible and newtonian fluid, the diffusion coefficient was considered as constant. The Navier-Stokes equation is shown according to the stream-vorticity formulation with species transport equation in a Finite Element Method approach.

The domain was discretized on an unstructured triangular mesh using the *GMSH* open source. Due to decoupling between velocity field and pressure field achieved by stream-vorticity formulation, the linear triangular element is a possible choice. The equations were discretized in space by Galerkin formulation and in time, the semi-Lagrangian scheme was used to discretized the material derivative using first order backward difference scheme.

The linear system of equations that comes from implementing the FEM is solved throught iterative method *Conjugate Gradient Solver* available in the public library for scientific tools *SciPy*. The dynamics of blood flow and species transport in coronary artery was investigated in two test cases as suggered by Wang *et al.* (2017) and the simulation was shown using *Paraview* open source.

2. MATHEMATICAL MODEL

A Finite Element Method approach is employed to analyse the dynamics of blood flow in coronary artery with atherosclerosis and possible influence of stents struts. The governing equations were developed according to continuum media assumption. Thus, the universal conservation laws such as conservation of mass, conservation of momentum and conservation of species transport were used in an Arbitrary Lagrangian-Eulerian context. The blood was modeled as single-phase, incompressible and newtonian fluid, the diffusion coefficiente was considered as constant. The Navier-Stokes equation is shown according to stream-vorticity formulation with species transport equation:

$$\frac{\partial \omega_z}{\partial t} + (\mathbf{v} - \hat{\mathbf{v}}) \cdot \nabla \omega_z = \frac{1}{Re} \nabla^2 \omega_z \tag{1}$$

$$\nabla^2 \psi = -\omega_z \tag{2}$$

$$\frac{\partial e}{\partial t} + (\mathbf{v} - \hat{\mathbf{v}}) \cdot \nabla e = \frac{1}{ReSc} \nabla^2 e \tag{3}$$

where, ω_z is the vorticity field, ψ is the stream function field, *e* is the concentration field, **v** is the material velocity field, $\hat{\mathbf{v}}$ is the mesh velocity field, ∇ is the Del operator, $Re = \rho u D/\mu$ is the Reynolds number, $Sc = \nu/D$ is the Schmidt number and *x* and *y* are the spatial variables. In addition to the material velocity field **v** is calculated by: $u = \partial\psi/\partial y$ and $v = -\partial\psi/\partial x$.

The boundaries conditions used were:

- *inflow condition*: this condition is specified when an mass inflow is desired. For such a condition, $u = u_o$ and $v = v_o$.
- *wall condition*: this condition is specified at wall boundaries (moving wall and noslip conditions). All the velocity components are specified with the same wall velocity values.
- *outflow condition*: this condition represents a state where is close to a fully developed profile. Usually no value is specified for the unknowns.
- *free-slip condition*: this condition is specified at the symmetric axis. The normal velocity component is null and the derivative of the tangent component is also null value.
- *strut condition*: this condition is used on the stent. The normal and tangential velocity components are specified with null value. The concentration field is specified as $c = c_o$.

As mentioned by Batchelor (1967), the ψ is constant along a streamline, then the streamfunction boundary condition can be calculated by $\psi_2 - \psi_1 = \int (udy - vdx)$, where can be used u and v velocity inflow component. In this work, was set null value for bottom streamline ψ_2. For top streamline ψ_1, it was calculated using u_o and v_o inflow velocity components, that is, $\psi_2 = \int (u_o dy - v_o dx)$. In addition, the vorticity boundary contition was calculated by $\omega_z = \nabla \times \mathbf{v}$ at each time step.

2.1 Galerkin Method

The domain was discretized on an unstructured triangular mesh using the *GMSH* open source. Due to decoupling between velocity field and pressure field achieved by stream-vorticity formulation, the linear triangular element can be used. The convective term of Eqs. 1 and 3 will be replaced by material derivative for further time discretization using semi-Lagrangian Method. For spatial discretization of governing equations, the Galerkin method was used, resulting in the following matrix system:

$$M\frac{D\omega_z}{Dt} + \frac{1}{Re}\Big[K_{xx} + K_{yy}\Big]\omega_z = 0 \tag{4}$$

$$-\Big[K_{xx} + K_{yy}\Big]\psi + M\omega_z = 0 \tag{5}$$

$$M\frac{De}{Dt} + \frac{1}{ReSc}\Big[K_{xx} + K_{yy}\Big]e = 0 \tag{6}$$

where, *M* is mass matrix, K_{xx} and K_{yy} are stiffness matrix.

2.2 Semi-Lagrangian Scheme

The Semi-Lagrangian Scheme in centred difference was proposed by Sawyer (1963) for atmospheric flow numerical simulation using vorticity-advection equation, allowing to use large time steps without numerical instability. However, because of a limited computer capability, the use of such methodology to model several fluid flow problems, with high order differences and fine mesh, came latter in the 1980's throught the work of Robert (1981) and Pironneau (1982), where the semi-lagrangian scheme would be able to run models faster than the Eulerian scheme, besides be unconditionally stable and only symmetric linear systems to solve. Basically, the semi-lagrangian scheme takes into account the fact that the Eulerian derivative is replaced by the material derivative, then it is discretized and computed along the trajectory characteristic:

$$\frac{D\omega_z}{Dt} \approx \frac{\omega_i^{n+1} - \omega_d^n}{\Delta t} \tag{7}$$

where, $D\omega_z/Dt$ is material derivative of ω_z and the right-hand side equation is material derivative discretized using first order backward difference scheme. The variable t is time, ω_i^{n+1} is the vorticity field calculated in current time step at the current node position and ω_d^n is the vorticity field calculated in previous time step at the departure node position.

The departure node is found by solving equation $\mathbf{x}_d^n = \mathbf{x}_i^{n+1} - \mathbf{v}\Delta t$, using the initial condition $\mathbf{x}_i^{n+1} = \mathbf{x}(t^{n+1})$ as shown in Figure 1a . A algorithm must be used to find the element that the departure node be, then the vorticity field in departure node (ω_d^n) is calculed by barycenter coordinates interpolation between nodes of element found. As shown in Figure 1b , three situations may occur depending on the trajectory: the first and the second situations are similar, differentiating only the trajectory length. In the first situation, the departure node is inside near element from current node, while the second situation the departure node is inside far element from current node. The third situation, the departure node is outside domain then the vorticity field in departure node receives the boundary condition value of nearest node to departure node.

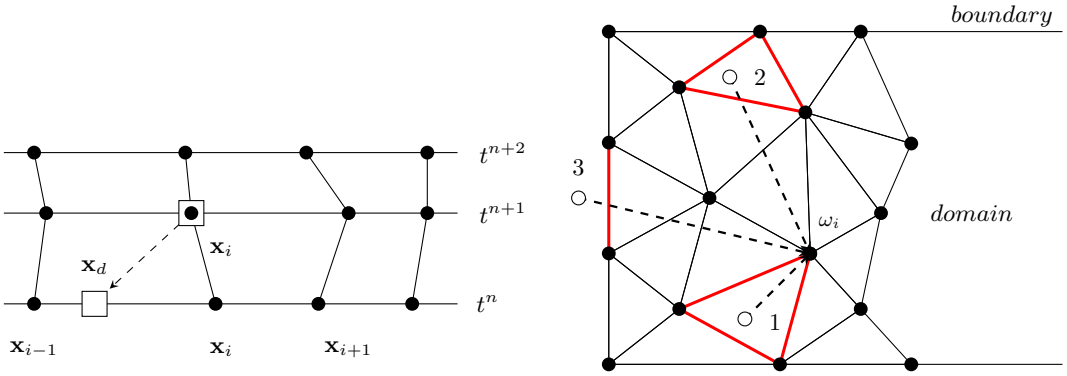

(a) (b)

Figure 1. In (a), an one-dimensional space scheme where the departure node x_d is found by integrating the mesh backward time. In (b), a two-dimensional space scheme where three situations may occur in searching procedure.

Therefore, the governing equations in matrix form used in this paper were:

$$\left[\frac{M}{\Delta t} + \frac{1}{Re}\left[K_{xx} + K_{yy}\right]\right]\omega_i^{n+1} = \frac{M}{\Delta t}\omega_d^n \tag{8}$$

$$\left[K_{xx} + K_{yy}\right]\psi = M\omega_z \tag{9}$$

$$\left[\frac{M}{\Delta t} + \frac{1}{ReSc}\left[K_{xx} + K_{yy}\right]\right]e_i^{n+1} = \frac{M}{\Delta t}e_d^n \tag{10}$$

whereas material velocity field $\mathbf{v}$ is calculated by: $u = G_y\psi$ and $v = -G_x\psi$, where G_y and G_x are the *Gradient global matrix*.

3. RESULTS AND DISCUSSION

In this section, we will present the results obtained from several cases with the numerical simulation of the Navier Stokes equation using the vorticity-streamfunction formulation with the species transport equation, where we have incompressible and monophase two-dimensional flow for all cases in an Arbitrary Lagrangian-Eulerian context using the

semi-Lagrangian Method. In all simulations, the computational mesh velocity is calculated using only the Laplacian smoothing velocity.

Initially, the *Poiseuille Symmetric* is shown, where the free slip condition is applied on the axis of symmetry and no-slip condition is applied in the top wall. Lastly, the results of numerical simulations for blood flow in a coronary artery are presented. The lumen radius of the coronary artery used was $R = 0.0015m$, the viscosity used was $\mu = 0.0035Pa.s$ and the density used was $\rho = 1060kg/m^3$ as suggested by Bozsak, Chomaz and Barakat (2014) Bozsak *et al.* (2014). According to Kessler et al. (1998) Kessler *et al.* (1998), the blood velocity in the coronary artery is $u = 12cm/s$. Thus, the Reynolds number used will be $Re = 54.5$.

The Navier-Stokes equation is used according to the vorticity-streamfunction formulation with the species transport equation for two geometries proposed by Wang et al. (2017) Wang *et al.* (2017), however modified to cartesian coordinates as shown in Fig. 3. In the section 3.2, the numerical simulation for the coronary artery with atherosclerosis and a drug-eluting stent in a curved channel model is presented for *Schmidt* number equal to 10. In the 3.3, the real coronary artery with atherosclerosis and a drug-eluting stent is also simulated with the same *Schmidt* number as in the previous section. Due to symmetry, only half of the domain is shown. The simulation was visualized using the *Paraview* open-source software proposed by Henderson (2007) Henderson (2007).

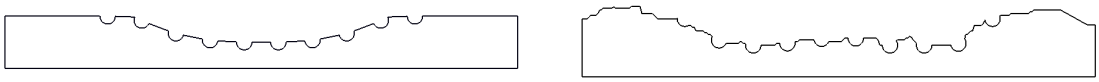

(a) Curved Channel (b) Real Channel

Figure 2. Non-dimensional domain for the blood flow in coronary artery The radius used was $R = 1$ and and the lumen length was $L = 10R$ as proposed by Wang *et al.* (2017)

3.1 Poiseuille Symmetric Flow

This section presents the simulation of the *Poiseuille* flow in half of the domain. Thus, the free-slip condition is required on the axis of symmetry. The Fig. 3. presents schematically this flow with the specified axis of symmetry and the expected velocity field.

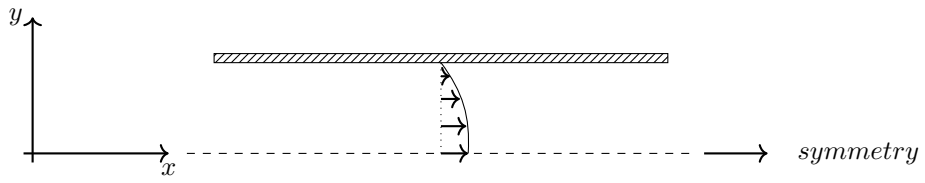

Figure 3. Half Poiseuille flow

The velocity profile equation is shown below:

$$u = u_{max}\big[1 - \frac{y^2}{L^2}\big] \tag{11}$$

where u_{max} is maximum velocity and its value is $u_{max} = 1.5$, L is non-dimensional length between the plates and its value is $L = 1$ and y is the vertical coordinates and it varies between $y = \big[0, 1\big]$. The domain was discretized using a linear triangular mesh with 3835 nodes and 7299 elements.

The Fig. 3. shows the unsteady velocity profile when $Re = 100$, in addition to the comparison between the numerical and analytical solutions in the steady state of proposed problem. It is possible to observe that the numerical solution converges to the analytical solution when the flow becomes steady state.

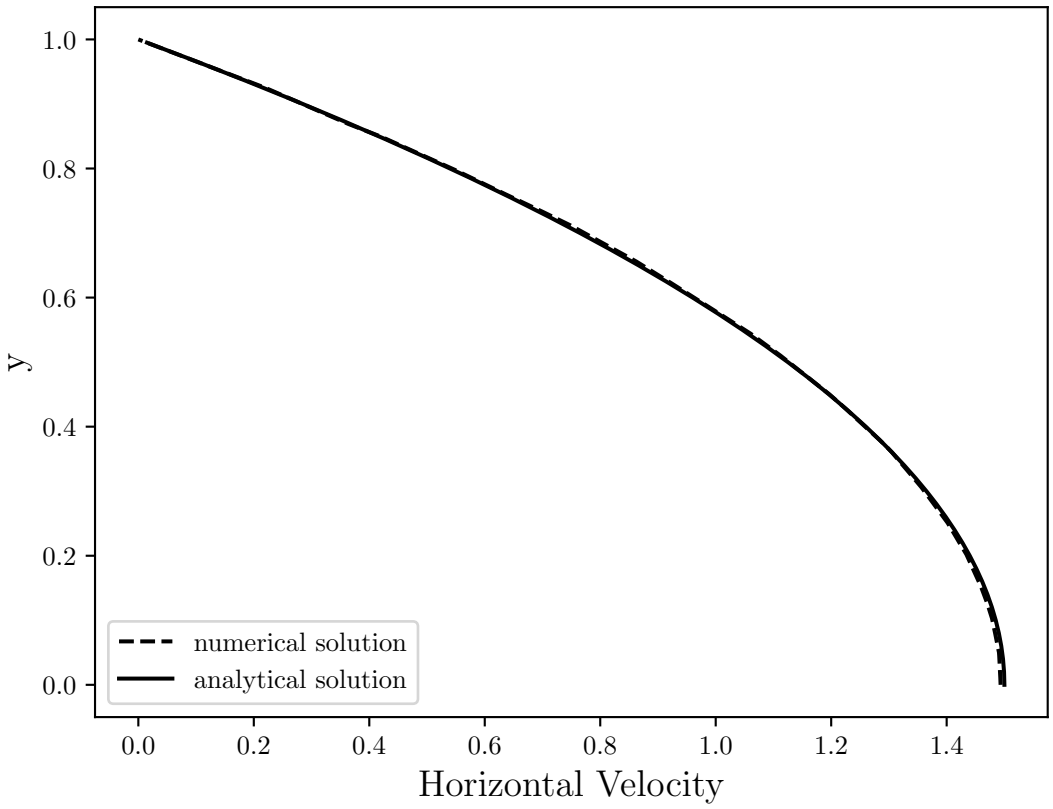

Figure 4. Unsteady velocity profile when $Re = 100$ and the comparison between the numerical and analytical solution for Half Poiseuille flow.

3.2 Curved Channel with Stent

In this section, will be present the case where the coronary artery has atherosclerosis and the drug-eluting stent is placed. It is modeled by 10 uniformly spaced semi-circles. The geometry used promotes a smooth reduction of the distance between the upper wall and symmetry axis of the channel. Due to atherosclerosis, 40% channel obstruction was considered and the domain was discretized using 15875 nodes and 35408 linear triangular elements.

The Fig. 3.2shows the unsteady state velocity profile in the middle section channel, that is, $x = 5.0R$. As expected, the numerical solution tends to a similar profile to the Half Poiseuille, as presented in the section 3.1. However, it is possible to observe an inversion of the velocity field sense at the top of the figure. This inversion occurs in the region that is located between the stents strut semi-circles. It is also possible to observe that the maximum horizontal velocity field in curvel channel reaches the $u = 3.43$ non-dimensional value, that is, more than 3 times the blood velocity in coronary artery without atherosclerosis and stent strut placed. This increase can influence the dynamics of blood flow and its biological processes and a more detailed analysis should be performed.

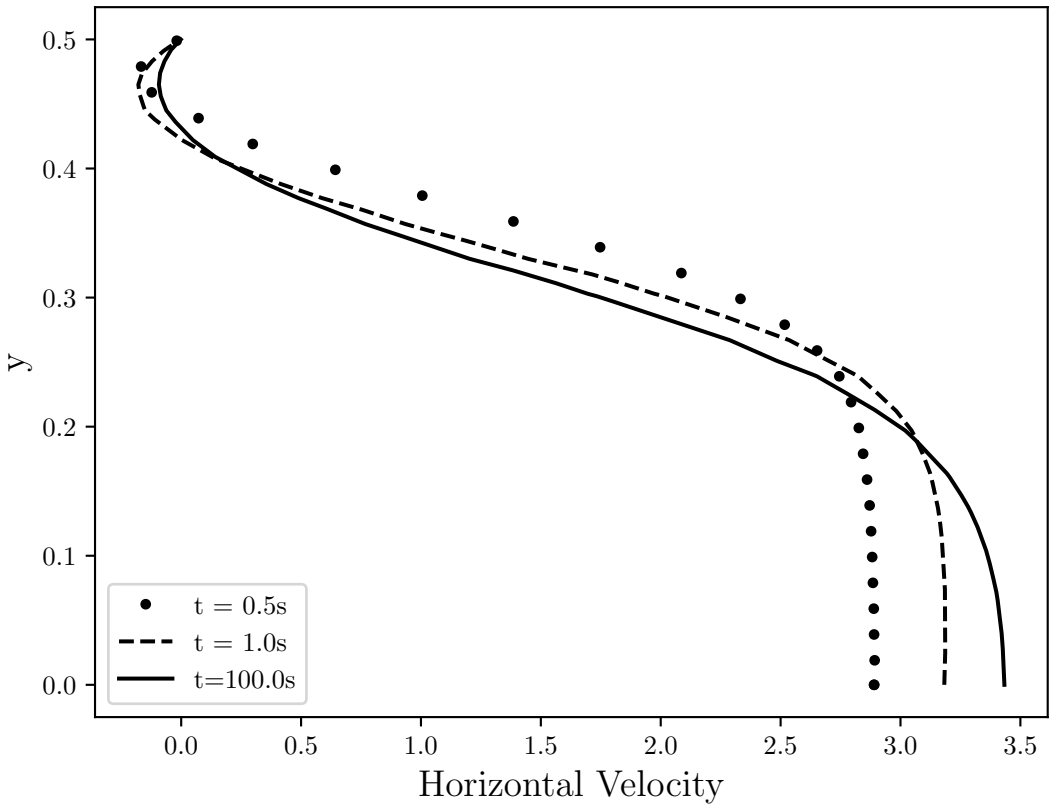

Figure 5. The unsteady state velocity profile in the middle ($x = 5.0R$) of the curved channel with drug-eluting stent.

The Fig. 3.2presents the evolution in time and space of the velocity field for half of the domain due to the symmetry of the solution. The velocity field is represented with non-dimensional values where the red color refers to the $u = 3.43$ value and the blue color $u = 0$ value. Conveting to dimensional values, we have $u = 41.16cm/s$ and $u = 0cm/s$ respectively. As can be seen, the region with the lowest horizontal velocity magnitude is found close to the boundary where the no-slip condition is applied. Whereas, it is increase close to the symmetric axis. Moreover, the largest horizontal velocity value is found in the maximum contraction region.

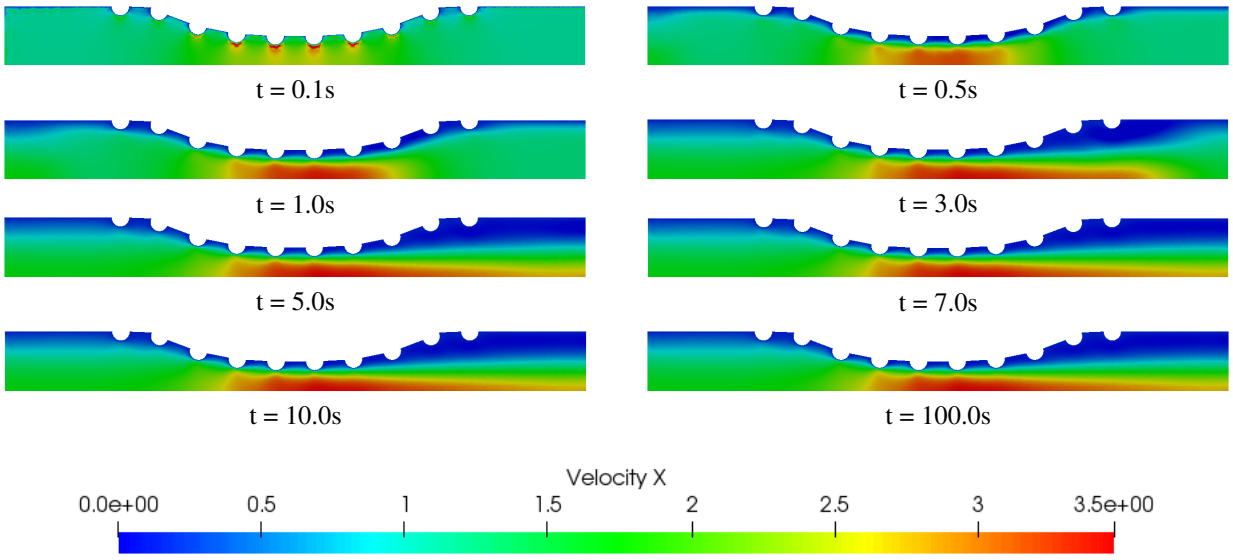

Figure 6. Temporal and spatial evolution of the velocity field for curved channel with drug-eluting stent.

As mentioned by Lucena et al. (2018) Lucena *et al.* (2018), it is estimated that 47% of the drug is diffused to the lumem and it is lost to the bloodstream. The Fig. 3.2shows the temporal and spatial evolution of the concentration field for the *Schmidt* number equal to 10. The concentration field is represented with the non-dimensional values where the red color represents 100% and the blue color represents 0% of the diffused concentration in the bloodstream.

It is possible to observe in the Fig. 3.2that the concentration field is more dispersed at the end of the curved channel due to the sense of the blood flow. It is possible that the drug concentration diffused affects the density and viscosity of the blood and consequently the Reynolds number. Thefore, the velocity field would also be affected. However, this influence is not considered in this work.

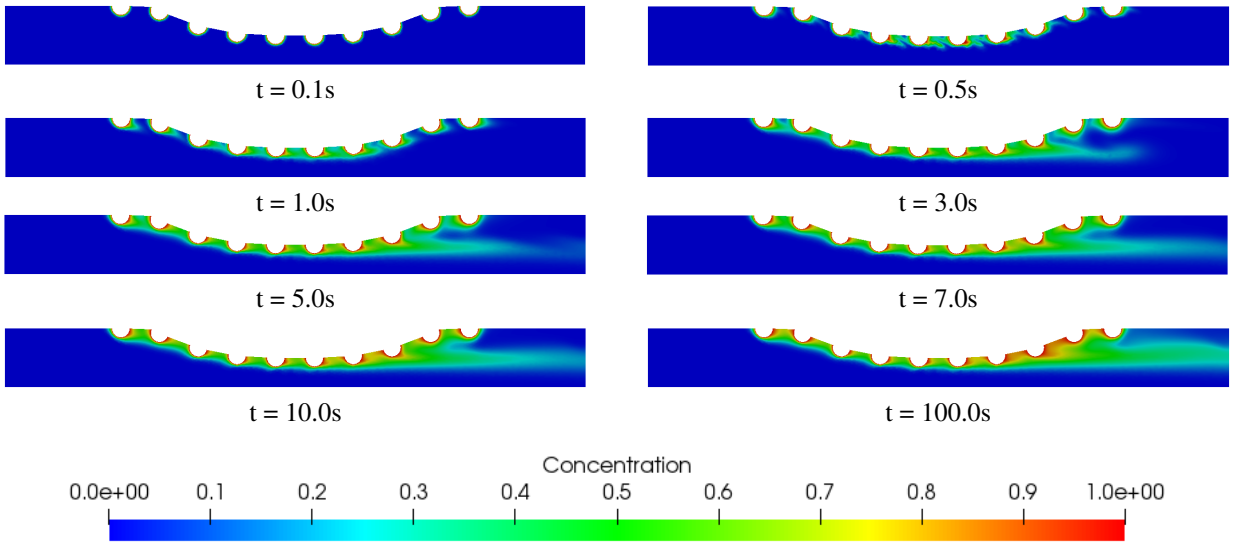

Figure 7. Temporal and spatial evolution of the concentration fiel for curved channel with drug-eluting stent and $Sc = 10$.

3.3 Real Channel with Stent

For this case, the numerical simulation is performed for a real coronary artery with atherosclerosis whose geometry was obtained through an image processing as suggested by Wang et al. (2017) Wang *et al.* (2017). This geometry is particular to each patient due to the patient health conditions. As in the previous case, the stent strut was modeled by 10 uniformly spaced semi-circles. The domain was discretized using 11807 nodes and 26426 linear triangular elements.

The Fig. 3.3shows the unsteady state velocity profile in the middle of the real channel, that is, $x = 5.0R$. Even so, the numerical solution shown a simular profile to the previous case, however it is not observed the inversion of the velocity field sense. It is also possible to observer that the maximum non-dimensional value of the velocity field reaches $u = 3.40$ close to symmetric axis. However, this velocity may vary according to the coronary artery geometry for each patient. It compared to the curved channel, the maximum horizontal velocity had a difference less than 1%. Therefore, the curved channel shown an acceptable approach, besides this model being simpler to implement and to perform the numerical simulations than real channel model.

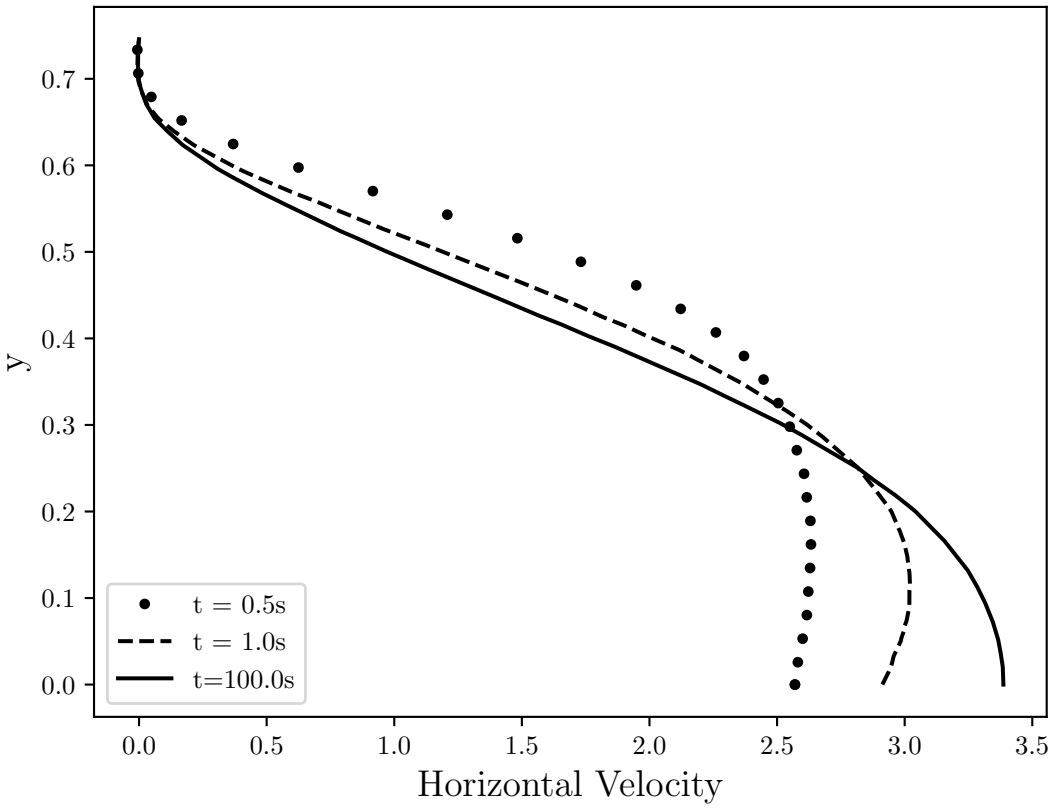

Figure 8. The unsteady state velocity profile in the middle of the real channel with drug-eluting stent.

The Fig. 3.3presents the evolution in time and space of the velocity field for half of the domain. The velocity field is represented with non-dimensional values where the red color refers to the $u = 3.40$ value and the blue color $u = 0$ value. Conveting to dimensional values, we have $u = 40.8cm/s$ and $u = 0cm/s$ respectively. As in the previous case, the region with the lowest horizontal velocity magnitue is found close to the boundary due to the no-slip condition and the largest horizontal velocity value is found close to symmetric axis. For this real channel, is possible to observe that there is two contraction region where the velocity field is increased. However, this coronary artery geometry varies for each patient and its blood dynamics can be changed.

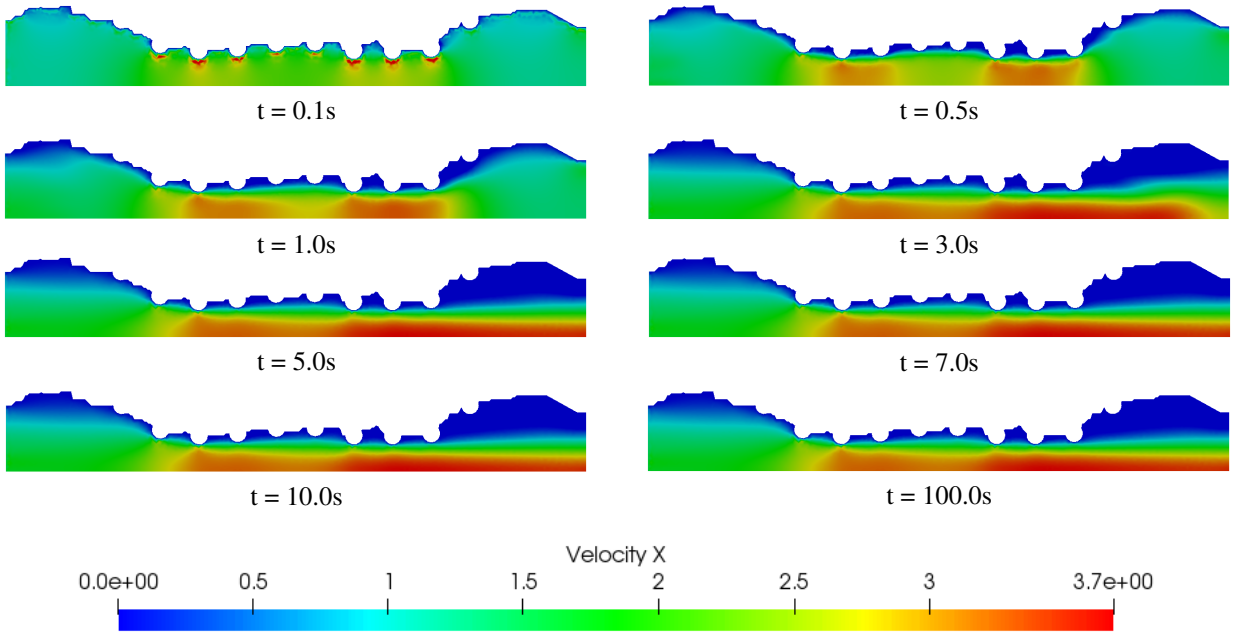

Figure 9. Temporal and spatial evolution of the velocity field for real channel with drug-eluting stent.

The Fig. 3.3shows the temporal and spatial evolution of the concentration field for the *Schmidt* number equal to 10. The concentration field is represented with the non-dimensional values where the red color represents 100% and the blue color represents 0% of the diffused concentration in the bloodstream. It is possible to observe that the concentration field dynamic is similar than the curved channel, no significant differences from the previous one Schmidt number. Only in some regions that the concentration field become more diffuse as a consequence of the velocity field decrease due to irregular geometry close to the semi-circles of the stents.

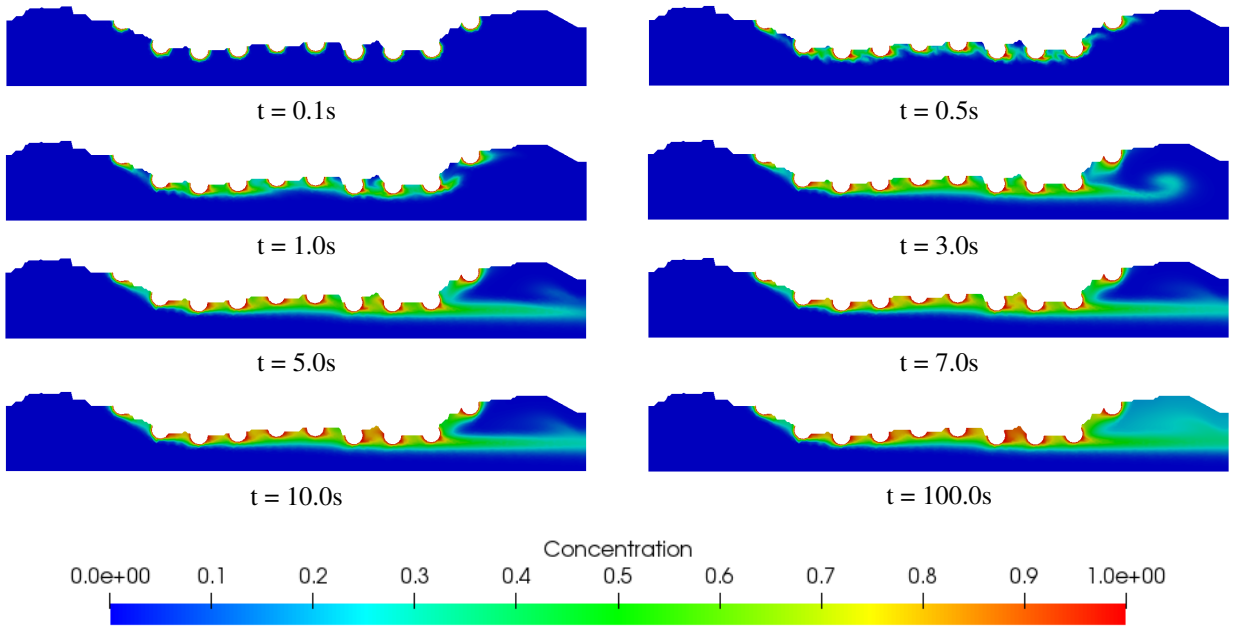

Figure 10. Temporal and spatial evolution of the concentration fiel for real channel with drug-eluting stent and $Sc = 10$.

4. CONCLUSION

In this work, a numerial code for Navier-Stokes equation according to the stream-vorticity formulation with species transport equation was developed using an ALE-FE approach. The semi-Lagrangian scheme was used to discretized the material derivative using first order backward difference scheme and the numerical oscillations were not seen for moderate to high Schmidt number.

The dynamics of blood flow was shown to a coronary artery with atherosclerosis and drug-eluting stent placed. It is possible to observe in the Fig. 3.2that the concentration field is more dispersed at the end of the curved channel due to the sense of the blood flow. It is possible that the drug concentration diffused affects the density and viscosity of the blood and consequently the Reynolds number. Thefore, the velocity field would also be affected. However, this influence is not considered in this work.

5. ACKNOWLEDGEMENTS

The authors thank the FAPERJ (Research Support Foundation of the State of Rio de Janeiro) for its financial support.

6. REFERENCES

Barquera, S., Tobias, A.P., Medina, C., Barrera, L.H., Domingo, K.B., Lozano, R. and Moran, A.E., 2015. "Global overview of the epidemiology of atherosclerotic cardiovascular disease". *Archives of Medical Research*, Vol. 46, No. 5, pp. 328 – 338.

Batchelor, G., 1967. "An introduction to fluid dynamics". *Cambridge University Press*.

Benjamin, E.J., Virani, S.S. and Callaway, C.W., 2018. "Heart disease and stroke statistics 2018 update: A report from the american heart association". *Circulation*, Vol. 137, No. 12.

Bozsak, F., J-M., C. and Barakat, A., 2014. "Modeling the transport of drugs eluted from stents: physical phenomena driving drug distribution in the arterial wall". *Biomech Model Mechanobiol*, Vol. 13, pp. 327–347. doi:10.1007/s10237-013-0546-4.

Henderson, A., 2007. "Paraview guide, a parallel visualization application". *Kitware Inc.*

Kessler, W., Moshage, W., Galland, A., Zink, D., Achenbach, S., Nitz, W., Laub, G. and Bachmann, K., 1998. "Assessment of coronary blood flow in humans using phase difference mr imaging comparison with intracoronary doppler flow measurement." *International Journal of Cardiac Imaging*.

Lucena, R., Mangiavacchi, N., Pontes, J., Anjos, G. and McGinty, S., 2018. "On the transport through polymer layer and porous arterial wall in drugâĂŘeluting stents". *Journal of the Brazilian Society of Mechanical Sciences and Engineering*.

Pironneau, O., 1982. "On the transport-diffusion algorithm and its applications to the navier-stokes equation". *Numerische Mathematik*.

Robert, A., 1981. "A stable numerical integration scheme for the primitive meteorological equations". *Atmosphere Oceans*, Vol. 19, pp. 35–46.

Sawyer, J., 1963. "A semi-lagrangian method of solving the vorticity advection equation". *Tellus*, Vol. 15, pp. 336–342.

Wang, H., McGinty, S., Lucena, R., Pontes, J., Anjos, G. and Mangiavacchi, N., 2017. "Dynamics of blood flow in coronary artery". *International Congress of Mechanical Engineering*.

World Health Organization, W., 2017. "Cardiovascular diseases". URL "www.who.int/cardiovascular_diseases/en/". [Online; accessed 03/05/2018 11:55].